nature COMMUNICATIONS

OPEN

ARTICLE

Received 14 Jan 2010 | Accepted 5 Mar 2010 | Published 12 Apr 2010

DOI: 10.1038/ncomms1009

The molecular network governing nodule organogenesis and infection in the model legume *Lotus japonicus*

Lene H. Madsen[1], Leïla Tirichine[1,†], Anna Jurkiewicz[1], John T. Sullivan[2], Anne B. Heckmann[1], Anita S. Bek[1], Clive W. Ronson[2], Euan K. James[3] & Jens Stougaard[1]

Bacterial infection of interior tissues of legume root nodules is controlled at the epidermal cell layer and is closely coordinated with progressing organ development. Using spontaneous nodulating *Lotus japonicus* plant mutants to uncouple nodule organogenesis from infection, we have determined the role of 16 genes in these two developmental processes. We show that host-encoded mechanisms control three alternative entry processes operating in the epidermis, the root cortex and at the single cell level. Single cell infection did not involve the formation of trans-cellular infection threads and was independent of host Nod-factor receptors and bacterial Nod-factor signals. In contrast, Nod-factor perception was required for epidermal root hair infection threads, whereas primary signal transduction genes preceding the secondary Ca^{2+} oscillations have an indirect role. We provide support for the origin of rhizobial infection through direct intercellular epidermal invasion and subsequent evolution of crack entry and root hair invasions observed in most extant legumes.

[1] Department of Molecular Biology, Centre for Carbohydrate Recognition and Signalling, Aarhus University, Gustav Wieds Vej 10, Aarhus C DK-8000, Denmark. [2] Department of Microbiology and Immunology, University of Otago, PO Box 56, Dunedin 9054, New Zealand. [3] EPI division, Scottish Crop Research Institute, Invergowrie, Dundee DD2 5DA, UK. †Present address: Génomique, Environnementale et Evolutive Section 3 CNRS UMR8197, Institut de Biologie de l'Ecole Normale Supérieure (IBENS), 46 rue d'Ulm, 75230 Paris Cedex 05, France (L.T.). Correspondence and requests for materials should be addressed to J.S. (stougaard@mb.au.dk).

Symbiosis between legumes and rhizobia is a non-pathogenic bacterial infection of a multicellular organism. Development of nitrogen-fixing root nodules is governed by a host genetic programme that synchronizes two processes running in parallel. Nodule primordia are formed from root cortical cells that re-initiate cell division, and simultaneously a bacterial infection process targets the developing primordia. This coordination has made separation of the molecular mechanisms underlying these two very different plant developmental processes difficult and has particularly limited the assignment of the specific role of plant genes governing bacterial infection. Adding further challenges to this analysis, microscopic investigation of a variety of wild and cultivated legume species has distinguished at least three different entry modes called infection thread invasion, crack entry and epidermal infection[1].

At the cellular level, infection of model legumes *Lotus japonicus (Lotus)* and *Medicago truncatula*, as well as crops such as soybean, pea and clover, is initiated when bacteria are entrapped by a curled root hair[2]. Local cell wall hydrolysis and invagination of the plasma membrane then lead to formation of infection threads that traverse to the base of the root hair cell. These plant-derived tubular structures proceed into the root cortex, branch and ramify in the nodule primordium[2]. Finally, rhizobia colonizing infection threads are released into plant cells, in which, surrounded by a peribacteriod membrane, they reduce atmospheric dinitrogen to ammonium. Continued containment of invading bacteria within specialized plant membranes is the characteristic feature of this intracellular invasion process.

Loss-of-function mutants in *Lotus* and *M. truncatula* have shown that perception of the rhizobial lipochitin-oligosaccharide (Nod-factor)[3,4] through Nod-factor receptors (NFR1 NFR5)[5–7] is required to trigger the earliest physiological responses to Nod-factor signals, Ca^{2+} influx, membrane depolarization and Ca^{2+} oscillations (spiking)[5,8], as well as for the initiation of nodule development[5–7]. Domain swaps and amino-acid substitutions have further suggested that the LysM domains of NFR1 and NFR5 receptors mediate the perception of bacterial Nod-factor and that recognition depends on Nod-factor structure[9]. The downstream signalling pathway is shared with mycorrhizal symbiosis and encompasses a leucine-rich repeat receptor kinase (*SymRK)*[10,11], cation channels (*Castor* and *Pollux)*[12–14], nucleoporins (*Nup85* and *Nup133)*[15,16], a calcium calmodulin-dependent protein kinase (*CCaMK)*[17–19] and a nuclear localized coil–coil protein (*Cyclops)*[20]. *SymRK, Castor*, *Pollux, Nup85* and *Nup133* function upstream of Ca^{2+} spiking, whereas *CCaMK* and *Cyclops* were suggested to decode the Ca^{2+} oscillation signature[17–19]. The current understanding is that the Nod-factor perceived at the plasma membrane through NFR receptors, accompanied by activation of the SYMRK receptor, leads to transmission of a secondary signal releasing calcium spiking in the nucleoplasm[21]. In turn, this calcium oscillation signature is decoded by nuclear-localized CCaMK[17–19]. Similarly, the nuclear membrane localization of CASTOR and POLLUX potassium channel proteins suggests a role in the regulation of calcium channels and in the release of calcium from the nuclear envelope[14]. Several alternative functions were suggested for nucleoporins, including import of secondary signal(s), anchoring of potassium channel proteins, transport of the NSP2 proteins mentioned below and regulation of calcium fluxes[15,16]. Further downstream of the shared pathway, putative transcriptional regulators of the NIN[22,23] GRAS (*Nsp1, Nsp2)*[24–27] and *ERF*[28,29] families are required for upregulation of nodule-expressed genes and initiation of nodulation[30,31]. Formation of nodule primordia involves dedifferentiation and reactivation of cortical root cells, and both gain-of-function and loss-of-function mutants have shown that cytokinin signalling through the cytokinin receptor (*Lhk1)*[32,33] is important for reactivation of the cell cycle in cortical cells. The genetic requirement for infection thread development is less well described but both the *Nap1* and *Pir1* genes that encode proteins of the SCAR/WAVE complex activating actin rearrangement in root hairs[34,] and *Cerberus*, which encodes a putative E3 ubiquitin ligase[35,] are required for normal infection thread progression. Mutational perturbation of most of the genes mentioned above leads to simultaneous absence of, or severe impairment of, organ formation and infection thread development. This has made the dissection of direct and indirect roles of the affected proteins within the two processes virtually impossible. Circumventing this obstacle, in this study, we have taken advantage of the two *Lotus* gain-of-function alleles, *snf1* and *snf2,* encoding a T265I calcium calmodulin-dependent kinase CCaMK[17,36,37] and a L266F cytokinin receptor LHK1[32,33,36,] respectively. These gain-of-function alleles uncouple organogenesis from infection and cause a development of empty spontaneous nodules in the absence of the bacterial symbiont, *Mesorhizobium loti* (*M. loti*), or bacterial Nod-factor signals. Using double, triple and quadruple mutants in the gain-of-function *snf1* and *snf2* genetic background, or transgenic roots, we have assigned genes and corresponding functions to separate paths or connecting cross-signalling functions in the complex molecular network controlling legume symbiosis. Altogether, the mechanistic role of 16 receptors and signal-transduction components previously characterized in a decade of gene discoveries was brought together in a synthesis defining a functional framework coordinating infection and organogenesis.

Results

Genes required for organogenesis and indirectly for infection. We assumed that NFR1 and NFR5 receptors would be necessary for rhizobial infection of spontaneous nodule primordia and therefore we first investigated the effect of *symrk*, *castor*, *pollux*, *nup133* and *nup85* loss-of-function mutations on the formation and infection of spontaneous nodules. Analysis of *SymRK* gene function is presented in detail to illustrate the approach (Table 1; Supplementary Fig. S1 online). To distinguish the role of the SYMRK receptor in infection and organogenic processes more precisely, we determined the impact of two loss-of-function non-nodulating alleles (*symrk-1* and *symrk-3*) caused by insertion of LORE retroelements[10] in an *snf1* genetic background, that is, in the presence of an autoactive CCaMK[17]. First, the effect on organogenesis was scored as the ability to form spontaneous nodules and, when no change in this capacity was observed, the effect on infection was subsequently scored as the frequency of pink functional nodules among the spontaneously formed non-functional white nodules. A set of *snf1* and *symrk* single mutants and *symrk snf1* double mutants were inoculated with *M. loti* on nitrogen-free agar slopes. As previously reported, *snf1* mutants developed fully infected nitrogen-fixing pink nodules with a high frequency, resulting in green plants and plant growth, whereas *symrk* mutants did not develop any nodules or nodule primordia and plants were nitrogen starved, yellow and did not grow (Table 1a; Supplementary Fig. S1). Spontaneous nodule primordia developed in *symrk snf1* double mutants. Unexpectedly, these spontaneous nodule primordia were also infected by *M. loti*, and nitrogen-fixing nodules, rescuing the non-nodulating and nitrogen-starved phenotype conferred by *symrk* mutations[10], were established (Fig. 1a–c, Table 1a, Supplementary Fig. S1). The frequency of pink nodules in *symrk-3 snf1* and *symrk-1 snf1* double mutants was relatively high, ~20% compared with 69% in *snf1* and 84% in wild type (Table 1a). This observation led us to determine whether the infections in *symrk snf1* mutants took place through root hair infection threads, that is, whether SYMRK was dispensable for infection thread formation in the presence of autoactive *snf1* CCaMK. Visualization of an *M. loti* strain constitutively expressing the β-galactosidase (*lacZ)* reporter gene showed invasion through root hair infection threads in *symrk snf1* mutants (Figs. 1d–k and 2a–f). However, emergence was delayed and the number was reduced

Table 1 | Frequency of infected pink nodules, presence of infection threads in root hairs and *trans*-cellular infection threads in nodule sections.

Plant line genotype	*M. loti* genotype	Pink nodules per total nodules		# of plants	ITs in root hairs	Average # of ITs in each nodule section
		Ratio	%			
(a) Gene functions required for organogenesis and indirectly for infection						
L. japonicus Gifu	Wild type	928/1102	84	309	+	28
snf1	Wild type	262/379	69	132	+	34
	None	0/443	0	154		
symrk-3snf1	Wild type	475/2590	18	411	+	32
symrk-1snf1	Wild type	34/163	21	48	+	
symrk-3	Wild type	0/0	0	100		
symrk-1	Wild type	0/0	0	70		
nup85-1snf1 21 °C	Wild type	111/222	50	64	+	28
nup85-1snf1 26 °C	Wild type	55/170	32	190	+	
nup85-1 21 °C	Wild type	2/8	25	40		
nup85-1 26° C	Wild type	0/0	0	49		
nup133-3snf1 21 °C	Wild type	140/646	21	306	+	49
nup133-3snf1 26° C	Wild type	50/205	24	191	+	
nup133-1 26 °C	Wild type	0/0	0	38		
castor-1 T265D CCaMK*	Wild type	44/106	41	11	+	30
*castor-1 control**	Wild type	0/0	0	8	–	
pollux-1 T265D CCaMK*	Wild type	39/128	30	37	+	
*pollux-1 control**	Wild type	0/0	0	16	–	
(b) Gene functions required for infection but dispensable for organogenesis						
nap1-1 T265D CCaMK*	Wild type	4/2217†	0.2†	48		
pir1-1 T265D CCaMK*	Wild type	1/903†	0.1†	31	+/–†	
*cerberus-3*T265DCCaMK*	Wild type	0/924	0	44	+/–†	
(c) Gene functions required for both infection and organogenesis						
nsp1-1 T265D CCaMK*	Wild type	1/17†,§	5.9†	15	–	
nsp2-3 T265D CCaMK*	Wildt type	0/0	0	57	–	
nin-2snf1	Wild type	0/0	0	115	–	
(d) Cross-talk between organogenesis and infection pathways						
ccamk-13snf2	Wild type	0/309	0.0	448	–	
ccamk-13	Wild type	0/0	0	50		
symrk-3snf2	Wild type	2/732	0.5	462	–	29
hit1-1snf1	Wild type	40/48†	83†	131	+	
cyclops-1 T265D CCaMK	Wild type	0/1028	0	56	–	
cyclops-2 T265D CCaMK	Wild type	0/2623	0	176	–	
snf2	Wild type	151/1101	13.6	313	+	14
snf2	None	0/446	0	60		
(e) Infection in absence of NFR1 and NFR5 receptors and/or in absence of Nod-factor signaling						
L. japonicus Gifu	nodC	0/0		250	–	
	nodA	0/0		100		
snf1	nodC	0/93	0	40		
	nodA	3/87	3.4	30		
har1-3snf1	nodC	23/508	4.5	57	–	
	nodA	3/531	0.85	54		
nfr1-1snf1	Wild type	11/337	3.2	208	–	
	nodC	2/270	0.75	189	–	
	nodA	9/315	2.8	205		
nfr5-2snf1	Wild type	6/82	7	96	–	
nfr1-1nfr5-2snf1	Wild type	25/572	4.3	501	–	10
	nodC	5/136	3.7	192	–	
	nodA	0/75	0	192		
nfr1-1nfr5-2-symrk-3snf1	Wild type	19/332	5.7	240	–	22
symrk-3snf1	nodC	0/472	0	117		
	nodA	0/393	0	115		
nfr1-1snf2	Wild type	0/613	0	131		
nfr5-2snf2	Wild type	0/997	0	201		

IT, infection thread; NFR, Nod-factor receptor.
*Hairy roots on mutant plants transformed with the control *CCaMK* wild-type gene did not differ from untransformed roots; for example, data presented for *castor-1* and *pollux-1*.
†Not significantly different from *hit1-1* mutant or untransformed *nsp1-1, pir1-1, nap1-1* and *cerberus-3* plants.
§Untransformed roots of *nsp1-1* forms small, uninfected nodule bumps in these experiments.

(five infection threads per wild-type root versus 0, and 55 versus 8, 1 and 2 weeks after inoculation, respectively). A closer inspection revealed infection threads in root hairs in close proximity to nodule primordia, and misguided infection thread growth associated with balloon-like swellings was not unusual (Figs. 1f and 2e–f). Light microscopy of thin sections of pink *symrk snf1* nodules shows infected cells completely or partly occupying the inner root nodule tissue (Fig. 1g–i) and an average of 32 *trans*-cellular infection threads per section compared with 28 in wild type (Table 1a). Confirming the light microscopy results, electron microscopy micrographs visualized infection threads in nodules with infected cells (Fig. 1j,k). Containment of bacteria within infection threads without release as reported in *SymRK/DMI2* RNA-mediated interference lines of *Sesbania* and *Medicago*[38,39] was not observed, implying that signal transduction through the SYMRK receptor was dispensable for root hair infection thread formation and bacterial release in *Lotus snf1* nodules.

Similar to *symrk* mutants, nucleoporin *nup133* and *nup85* mutants and potassium channel *pollux* and *castor* mutants show limited root hair responses to *M. loti* and lack the calcium-spiking characteristic for Nod-factor-induced signalling[8,12–16]. As previously reported, the inoculation of *nup133* and *nup85* mutants with *M. loti* resulted in a temperature-dependent non-functional and reduced infection phenotype[15,16]. In contrast, *nup133 snf1* and *nup85 snf1* double mutants were invaded through root hair infection threads and nitrogen-fixing nodules developed to rescue the ineffective nodulating phenotype of the single mutants at both the normal 21 °C growth conditions and the non-permissive 26 °C (Table 1a; Figs. 2g–l, 3 and 4; Supplementary Fig. S1). Infection threads were observed in root hairs in proximity to nodule primordia (Fig. 2g–j). Comparable infections of the non-nodulating *castor* and *pollux* mutants were observed using a dominant T265D version of CCaMK and transgenic roots generated by *Agrobacterium rhizogenes*-mediated transformation (Table 1a).

Genes required for infection but dispensable for organogenesis. *nap1*, *pir1* and *cerberus* mutant plants have all previously been shown to develop nodule primordia with aberrant infection thread formation or progression[34,35]. To extend the infection thread observations, we transformed these mutants with the T265D construct of CCaMK. The phenotype of arrested infection threads and lack of infected nodules in the mutant plants transformed with T265D CCaMK confirmed that *Nap1*, *Pir1*[34] and *Cerberus*[35] genes function in the infection thread pathway (Table 1b).

Gene functions required for both infection and organogenesis. Previous characterization of *nin*, *nsp1* and *nsp2* mutants suggests a function for these transcriptional regulators in both infection and organogenesis[22–27]. The lack of spontaneous nodules observed in *nin-2 snf1* double mutants, as well as the unchanged phenotype of *nsp1*and *nsp2* mutants, transformed with the T265D CCaMK construct confirmed their role in organogenesis. Microscopy of roots inoculated with the *M. loti lacZ* strain detected root hair deformations but no infection threads in *nin-2 snf1* double mutants (Table 1c). The impaired infection and organogenesis phenotype were also unchanged in the *nsp1* and *nsp2* mutants transformed with the T265D variant of CCaMK (Table 1c).

Cross-talk between organogenesis and infection pathways. The availability of corresponding gain-of-function (*snf1*, *snf2*)[17,32] and loss-of-function (*ccamk*, *hit1*)[17,33] mutants of *CCaMK* and the *Lhk1* cytokinin receptor genes enabled us to investigate the interdependence of organogenesis and root hair infection. Infection of reciprocal *snf1 hit1* and *ccamk-13 snf2* double mutants was analysed, together with *symrk-3 snf1* and *symrk-3 snf2* mutants. Inactivation of CCaMK in *ccamk-13 snf2* resulted in an absence of infection of the spontaneously formed primordia caused by *snf2* gain-of-function cytokinin receptor activity. In addition, inactivation of the SYMRK receptor in *symrk-3 snf2* mutants resulted in a very low infection frequency of *snf2*-induced spontaneous nodules compared with the autoactive CCaMK-induced primordia in *symrk-3 snf1* double mutants (Table 1d and a). Together, these results indicate a role for activated CCaMK in cross-signalling between the organogenic and root hair infection thread pathways and a role for SYMRK in the signalling leading to CCaMK activation. In the reciprocal combination of the loss-of-function cytokinin receptor, *hit1,* and the autoactive CCaMK in *hit1 snf1* double mutants, an excessive infection thread formation comparable to the level observed in *hit1* mutants was detected. As previously observed for *hit1* mutants[33], *hit1 snf1* mutants show reduced nodulation, whereas organogenesis was absent in uninoculated plants (see Supplementary Table S1). The simplest conclusion from these two sets of experiments is that cross-signalling to the root hair infection pathway is CCaMK dependent and that cytokinin signalling mediated by the downstream-functioning *snf2* gain-of-function cytokinin receptor was unable to activate the infection thread pathway effectively. See Supplementary Table S1 for the analysis documenting that CCaMK functions upstream of the LHK1 cytokinin receptor. We infer that cross-signalling through CCaMK seems to enhance the efficiency of nodule primordia infection and that cell division alone as in *snf2* mutants is insufficient. CYCLOPS was recently suggested to function in the infection pathway and was shown to interact directly with CCaMK[20,40]. Our inspection of nodules on *cyclops* roots transformed with the T265D CCaMK construct confirms the absence of infection and infection threads in *cyclops* mutants (Table 1d), suggesting that CYCLOPS is important for CCaMK cross-signalling from the organogenic to the infection pathway. Previous experiments using a CaMV 35S promoter to drive T265D CCaMK expression resulted in organogenesis beyond the primordial stage, showing that CYCLOPS is dispensable for organogenesis[20]. In our experiments using the cognate CCaMK promoter, this is less obvious and a level of CYCLOPS-dependent back signalling from the infection pathway cannot be excluded.

Infection in the absence of NFR1 and NFR5 receptors. To determine the requirement for host Nod-factor perception in the intracellular root hair infection thread pathway, double, triple and quadruple mutants of *Nfr1*, *Nfr5* and *SymRK* receptors unable to perceive the Nod-factor signal, and/or impaired in downstream signal transduction, were inoculated with *M. loti*. To our surprise, pink nodules developed in *nfr1-1 snf1* and *nfr5-2 snf1* double mutants, as well as in *nfr1-1 nfr5-2 snf1*, *nfr1-1 nfr5-2 symrk-3 snf1* triple and quadruple mutant plants, although at 10- to 20-fold lower frequencies than in *snf1* and wild-type plants (Figs. 4a, h–q and 5; Table 1e). Both normal pink nodules and pink sectored nodules were observed (Fig. 4b, c, and l–t). Most plants carrying these nodules displayed dark green leaves and grew, indicating nitrogen fixation in the nodules (Fig. 5a,b). Microscopy revealed that infected cells in sectored nodules were not distributed evenly (Fig. 4m, o and q) as seen in wild type and most but not all *snf1* nodules (Fig. 4a,h,i). The invasion process was therefore followed using *M. loti* strains expressing enhanced green fluorescent protein (eGFP) or *lacZ*. Using fluorescence and light microscopy, we were unable to detect infection threads in root hairs of *nfr1-1 snf1*, *nfr5-2 snf1*, *nfr1-1 nfr5-2 snf1* and *nfr1-1 nfr5-2 symrk-3 snf1*, but thin sections of nodules revealed *trans*-cellular infection threads in the central nodule tissue (Fig. 3a–c). Infection threads were also observed in electon microscopy micrographs (Fig. 3d–f). Thin sections of fully or partly infected nodules indicate that these were invaded through infection threads initiated by *M. loti* entering through cracks at the junctions of nodules and roots, followed by bacterial accumulation in intercellular pockets (Figs. 3g and 4r–t). In contrast to the corresponding *snf1* double

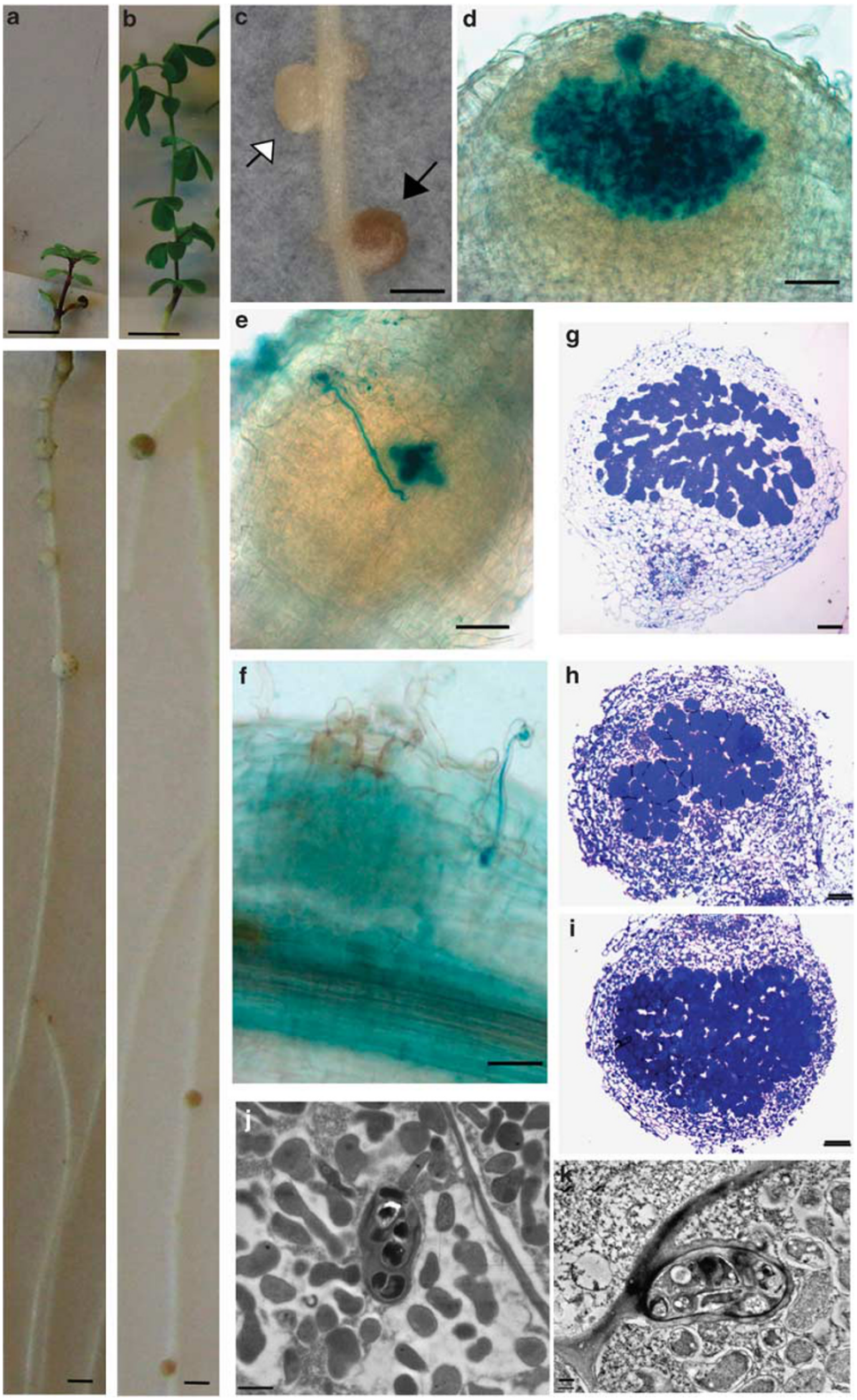

Figure 1 | Infection of spontaneous nodules and development of nitrogen-fixing root nodules on *symrk-3 snf1* mutants. (**a**) Spontaneous nodules on uninoculated plant. (**b**) Nitrogen-fixing pink nodules on *M. loti*-inoculated plant. Roots are shown close-up to visualize nodules. (**c**) Close-up of root nodules. Closed arrow: infected pink nodule, open arrow: white uninfected nodules. (**d**, **e**) Infection of primordia visualized by staining of *M. loti::lacZ* bacteria within infection threads. (**f**) Root hair infection thread. (**g**) Thin section of wild-type control infected by *M. loti*. (**h**, **i**) Thin sections of a partly and fully infected pink nodule. (**j**, **k**) EM of infection threads in *M. loti*-infected nodules. Size bars: (**a**, **b**): upper (shoot) part: 1 cm; lower (root) part: 1 mm, (**c**): 1 mm, **d**–**f**: 20 μm, **i**: 200 μm, **h**: 100 μm, **j**: 1 μm, **k**: 1 μm.

mutants, no infected pink nodules were observed in *nfr1-1 snf2* and *nfr5-2 snf2* mutants inoculated with *M. loti* (Table 1e).

Infection in the absence of Nod-factor signalling. To further investigate the role of the Nod-factor signal in this alternative intercellular entry process, a set of *symrk-3 snf1*, *nfr1-1 snf1* and *nfr1-1 nfr5-2 snf1*, as well as a *har1-3 snf1* hypernodulating mutant, which is impaired in the shoot regulation of nodule numbers by the HAR1 receptor kinase, were inoculated with *M. loti nodC* or *nodA* mutants unable to synthesize functional Nod-factors[41]. In *symrk-3 snf1* mutants, no infected nodules were observed (Table 1e), but interestingly, infections were observed in *nfr1-1 snf1*, *nfr1-1 nfr5-2 snf1* and *snf1 har1* mutants even in the absence of Nod-factor and NFRs. Compared with wild-type and *snf1* plants, infection frequencies were reduced 20- to 100-fold (Table 1e). Almost all of these pink nodules were sectored and showed irregular morphologies (Figs. 4d-g, 5c,d). Using fluorescence and light microscopy and *M. loti* strains expressing eGFP or *lacZ*, we were unable to detect infection threads in root hairs or *trans*-cellular infection threads. Inspection of thin sections of nodules of *nfr1-1 snf1* and *nfr1-1 nfr5-2 snf1* mutants inoculated with *nodC* or *nodA* mutants (Figs. 3h and 5e,f) indicates that infection of these nodule primordia occurs through intercellular epidermal entry and shows an anatomy in which only few cells, often only single cells, are infected (Fig. 5e–g). These infected cells seem enlarged compared with infected cells in wild-type nodules, suggesting size regulation in wild-type nodules. Infected cells that had recently divided were also observed (Fig. 5f–g). Extending the analysis using transmission electron microscopy (TEM), the absence of *trans*-cellular infection threads was confirmed. TEM micrographs, similar to fluorescence and light microscopy, only reveal intercellularly located bacteria and bacteria inside infected cells (Fig. 3i). Among all the sections obtained, two images show sub-cellular structures most likely representing the invasion mechanism operating at the single cell level (Fig. 3j–l). The thin section (Fig. 3j) shows an intracellular infection that seems to be connected to an adjacent intercellular pocket of bacteria. The TEM micrograph (Fig. 3k,l) shows a comparable infection structure. Here, an intercellular pocket of bacteria is located adjacent to an intracellular infection peg that seems to enlarge into a butterfly-shaped release structure containing numerous bacteria. We infer that these expanded intracellular infection pegs are induced by bacterial entry from the intercellular pocket and we propose to call this path for single-cell peg entry. In support of this interpretation, comparable short infection structures originating from intercellular bacteria were observed in lupinoid root nodules[42,43].

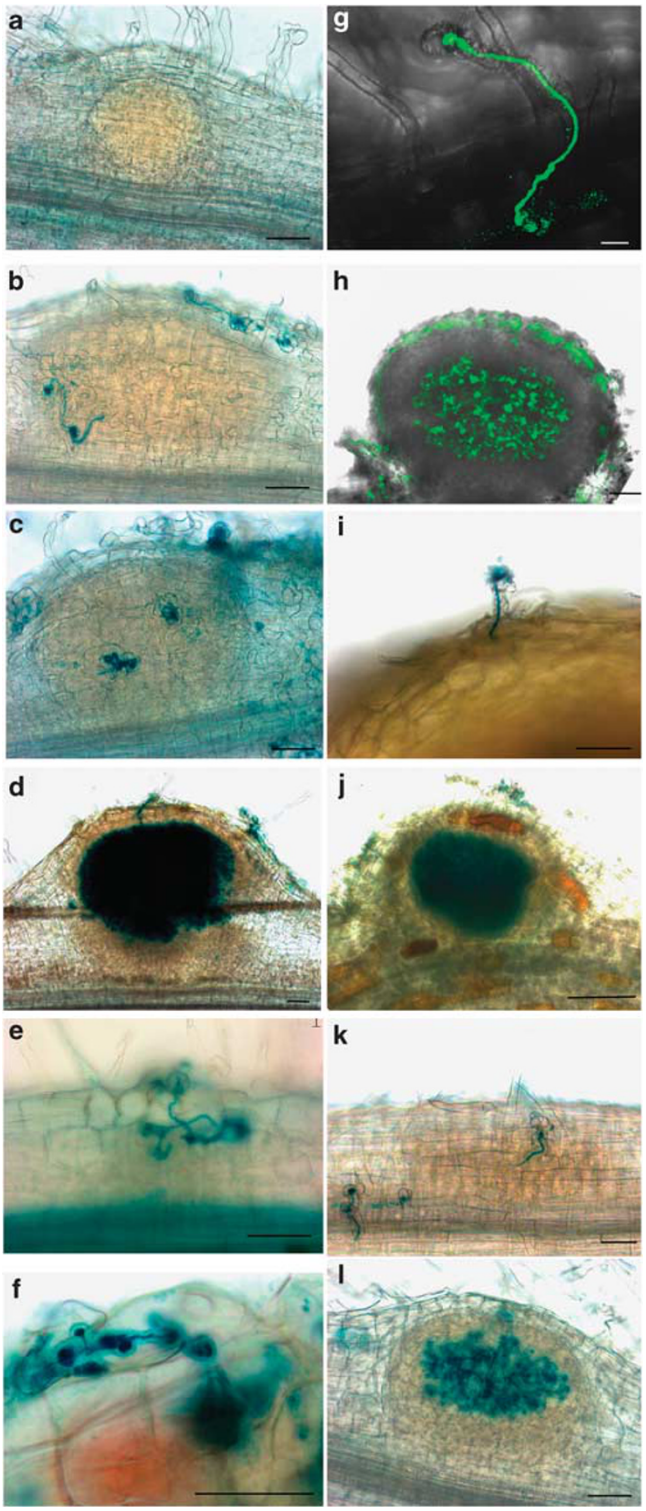

Discussion

The results presented here define the components of two parallel pathways facilitating infection thread formation and root nodule organogenesis, respectively (Fig. 6a). We have shown that the SYMRK receptor, the two nucleoporins (NUP133, NUP85) and the potassium channels (CASTOR and POLLUX) involved in signal transduction downstream of Nod-factor perception are dispensable for root hair infection thread development and invasion of nodule primordia in an *snf1* genetic background. On the other hand, NFRs (NFR1 and NFR5) were required for root hair infection thread initiation, and NAP1 and PIR1 mediating actin rearrangement, together with the putative ubiquitin E3 ligase (CERBERUS), were required for infection thread progression. A simple explanation is an early branching of the NFR and Nod-factor-mediated signal transduction (Fig. 6a). NIN, NSP1 and NSP2 transcriptional regulators were

Figure 2 | Infection of spontaneously induced nodule primordia in double mutants. (**a–f**) *symrk-3 snf1* nodules. (**a**) Uninfected primordium. (**b**, **c**) Examples of bacteria in infection threads approaching a spontaneous nodule primordium. (**d**) Old, fully infected nodule. (**e**, **f**) Close-up of partly misguided infection threads with swellings. (**g**) Infection thread in *nup85-1 snf1* root hair. (**h**) Fully infected *nup85-1 snf1* nodule. (**i**) Infection thread in *nup133-3 snf1* root hair above spontaneous nodule primordium. (**j**) Fully infected *nup133-3 snf1* nodule. (**k**) Infection thread in *L. japonicus* wild-type root hair above nodule primordium. (**l**) Young, fully infected wild-type nodule. Infection threads and infected tissue were visualized by staining of *M.loti* bacteria expressing *lacZ* (**a–f** and **i–l**) or by fluorescence of *M. loti* bacteria expressing eGFP (**g–h**). Scale bars (**a–g**, **i**, **k**, **l**): 20 μm, (**j**): 50 μm, (**h**): 100 μm.

required for both infection and organogenesis, supporting a role in both infection thread formation and cortical cell activation. Our results further indicate that calcium spiking by itself is dispensable for infection thread formation, as inactivation of SYMRK, nucleoporins (NUP133, NUP85) and potassium channels (CASTOR and POLLUX) results in an absence of calcium spiking[8]. At the same time, a presumed Ca^{2+} activation of CCaMK, as mimicked by the *snf1* mutation, seems insufficient for root hair infection thread formation, as functional NFR1 and NFR5 receptors were required for root hair infection thread formation in *snf1*. Together this suggests that the NFR receptor-dependent Ca^{2+} influx observed in root hairs at high Nod-factor concentration or other, as yet undiscovered, NFR-dependent early responses may be a prerequisite for root hair infection thread formation. Supporting these interpretations, observation of morphological root hair responses in *M. truncatula* mutants, corresponding to our *Lotus symrk*, *castor*/*pollux* and *ccamk* mutants, also suggests a separate pathway leading to root hair curling[44].

Absence of infection of *cyclops* primordia after expression of a T265D CCaMK from the CaMV 35S promoter[20] and in our experiments from the CCaMK promoter, together with the reported protein–protein interaction between CCaMK and CYCLOPS, indicates a role for CYCLOPS in cross-signalling between organogenic and infection pathways[20,40]. The ineffective invasion in the *snf2* mutant background supports this notion and indicates that component(s) responsible for cross-signalling from the organogenic pathway to the infection pathway depend on CCaMK activity while acting upstream of cytokinin responses. In accordance with this interpretation, the *hit1snf1* double mutants inoculated with *M. loti* formed infection threads, whereas *ccamk-13 snf2* mutants did not. We suggest that the delayed and the two- to threefold lower infection frequency observed in *symrk*, *nup133*, *nup85*, *castor* and *pollux* mutants within the *snf1* background may result from a lack of synchronization between organogenesis and infection, leading to misguidance of infection threads as seen in *hit1* mutants[33]. Alternatively, ineffective cross-signalling though autoactive CCaMK proteins may lead to a lower infection frequency. Similarly, lack of synchronization was suggested to explain the delayed nodulation in inoculation of *Sesbania* plant with a mixture of rhizobial mutant strains[45].

Our results uncover unusual intercellular infection processes in the normally intracellularly root hair-infected *Lotus* plants (Fig. 6b). Intercellular infection and formation of *trans*-cellular infection threads within the root nodules occurred in the absence of functional NFR1 and NFR5 receptors, although at 10- to 20-fold lower frequencies than in *snf1* and wild-type plants. Nevertheless, a comparison of infection thread formation induced by wild-type *M. loti*

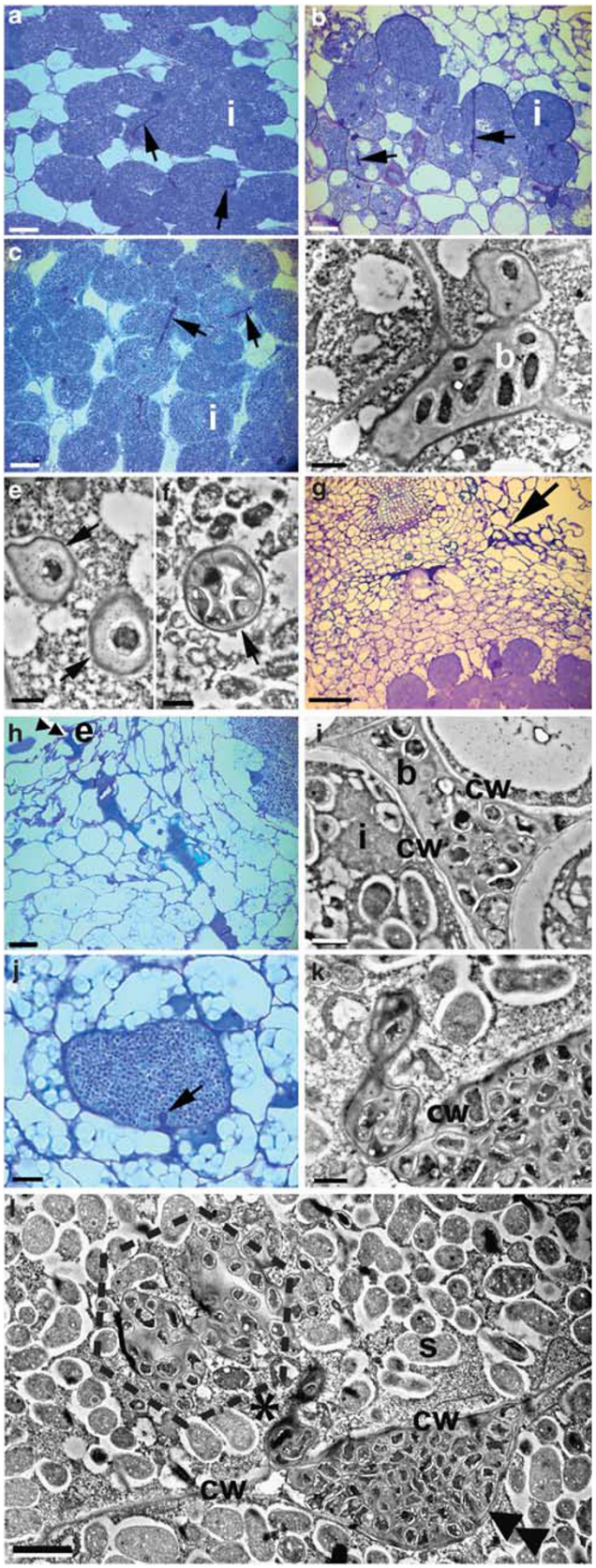

Figure 3 | Intercellular infection mechanisms. (**a**) Control showing *trans*-cellular infection threads (ITs) in thin section of *M. loti*-infected wild-type nodule. Arrows: ITs; (**b**) *trans*-cellular ITs (arrows) in *nfr1-1nfr5-2 symrk-3 snf1* nodule infected by *M. loti*; (**c**) *trans*-cellular ITs (arrows) in *symrk-3snf1* infected by *M. loti*. (**d**) and (**e**) Transmission electron microscopy (TEM) micrograph of ITs (arrows) in *M. loti*-infected wild-type nodule. (**f**) Infection thread (arrow) in *M. loti*-infected *nfr1-1 nfr5-2 symrk-3 snf1* nodule. (**g**) Crack entry (arrow) of *M. loti* into *nfr1-1 nfr5-2 symrk-3 snf1* nodule. (**h**) Intercellular epidermal infection of *nodC* mutant bacteria into an *nfr1-1 nfr5-2 snf1* nodule. Double arrow: bacterial entry point. e: Epidermal cell. (**i**) Intercellular *nodC* bacteria inside *nfr1-1 nfr5-2 snf1* nodule. cw: Cell wall, b: bacteria. (**j**) Single cell infection in an *nfr1-1 nfr5-2 snf1* nodule. Infection thread (arrow) initiated by intercellular *nodC* bacteria (double arrowhead). (**k**) Close-up of infection thread marked by a * in (**l**): a short infection thread initiated from an adjacent pocket of intercellular *nodC* bacteria in an *nfr1-1 nfr5-2 snf1*nodule. cw: Cell wall. (**l**) Enlarged infection thread release structure in an *nfr1-1 nfr5-2 snf1* nodule infected by *nodC*. Hexagon (dashed line) surrounds the butterfly-shaped release structure. *Infection thread, cw: cell wall, double arrowhead: pocket of intercellular bacteria, i: infected cell, s: symbiosome. Size bars **a–c**: 20 µm, **d**, **i**, **k**, **l**: 1 µm, **e**,**f**: 500 nm, **g**: 50 µm, **h**: 10 µm, **j**: 5 µm.

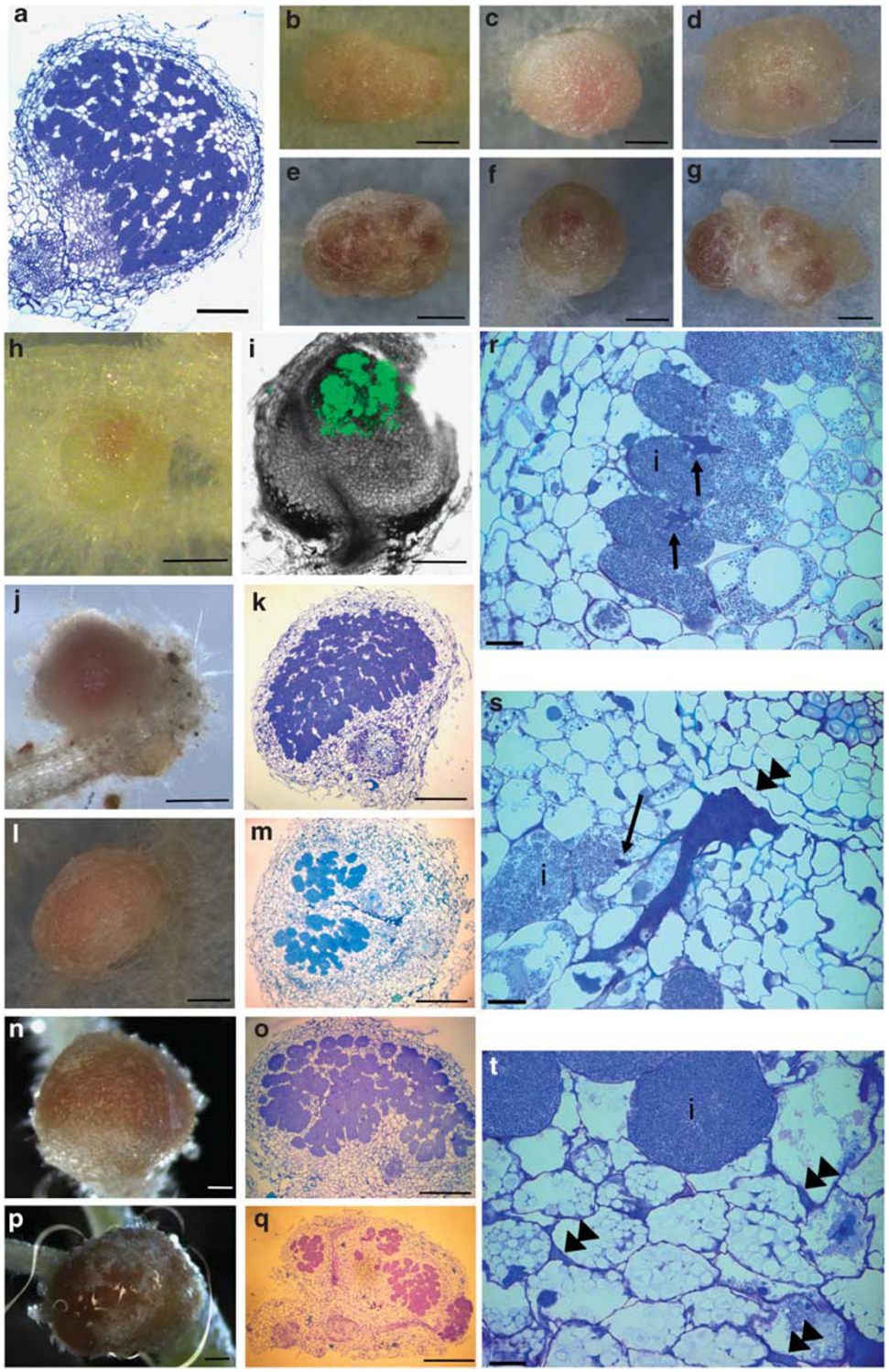

Figure 4 | Examples of nodule morphologies and thin sections of infected spontaneous nodules. (**a**) Thin section of a fully infected *M. loti* nodule on an *snf1* plant, (**b**) *nfr1-1 snf1* infected with *M. loti*, (**c**) *nfr5-2 snf1* infected with *M. loti*, (**d**) *har1-3 snf1* infected with *nodC*, (**e**) *har1-3 snf1* infected with *nodA*, (**f**) *har1-3 snf1* infected with *nodC*, (**g**) *har1-3 snf1* infected with *nodC*, (**h**) *snf1* infected with *M. loti* expressing eGFP, (**i**) fluorescence microscopy of a thin section of nodule in (**h**), (**j**) *nup85-1 snf1* infected with *M. loti*, (**k**) thin section of nodule in (**j**), (**l**) *nfr1-1nfr5-2 snf1* infected with *M. loti*, (**m**) thin section of nodule in (**l**), (**n**) *nfr1-1 nfr5-2 symrk-3 snf1* infected with *M. loti*, (**o**) thin section of nodule in (**n**), (**p**) *nfr1-1 nfr5-2 symrk-3 snf1* infected with *M. loti*, (**q**) thin section of nodule in (**p**), (**r, s, t**) thin sections of nodules of *nfr1-1 nfr5-2 symrk-3 snf1* infected with *M. loti*. i: infected cell, double arrowheads: pockets of intercellular bacteria, arrows: infection threads, emerging from pockets. Size bars (**a**), (**i**), (**k**), (**m**), (**o**), (**q**): 200 μm; (**b–h**), (**j**), (**l**): 500 μm; (**n**) and (**p**): 200 μm; (**r–t**): 5 μm.

and *nodC* mutants shows that synthesis of the bacterial Nod-factor was required for the effective development of these *trans*-cellular nodule infection threads. The mechanism involved in such a cortical perception is unknown, but involvement of one or more of the 15 additional receptor kinases belonging to the *Lotus* NFR1 and NFR5 families is conceivable[46]. Six of these family members, *Lys2*, *Lys3*,

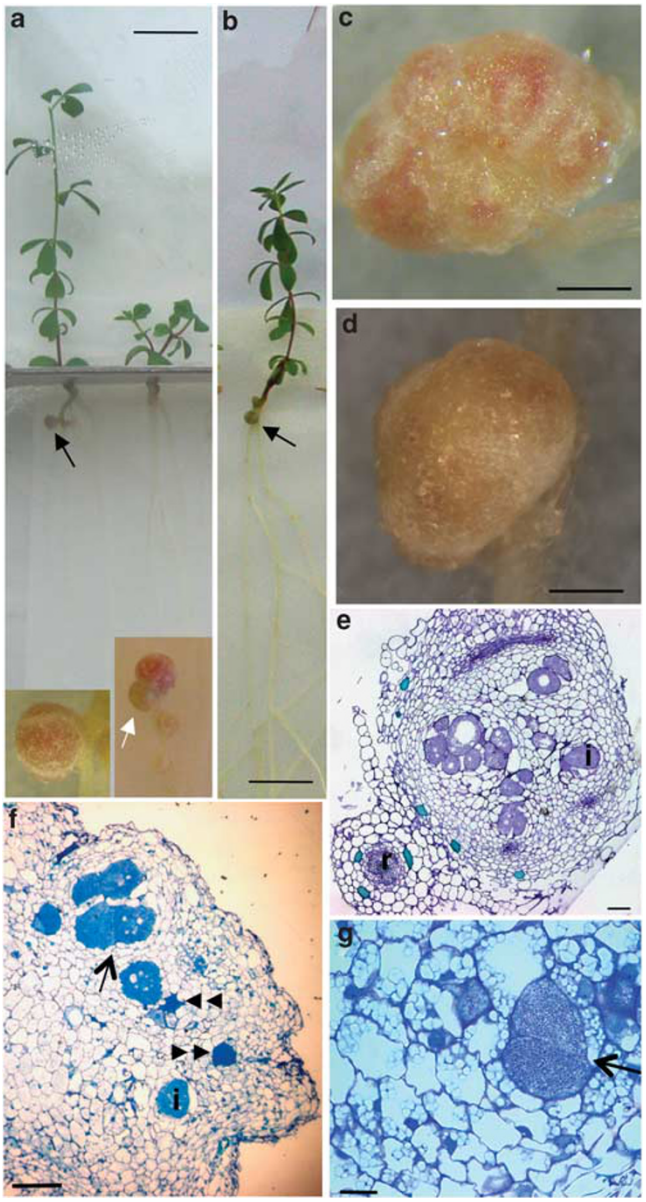

Figure 5 | Infection of spontaneously induced nodule primordia in the absence of Nod-factor receptors and/or Nod-factor. Development of nitrogen-fixing nodules (black arrows) on (**a**) *nfr1-1snf1* and (**b**) *nfr5-2snf1* double mutants inoculated with *M. loti*. Inset: Close-up of infected *nfr1-1snf1* nodules. White arrow marks uninfected nodule. (**c**, **d**) Partially infected spotted nodules on (**c**) *nfr1-1snf1* infected by *nodA* and (**d**) *nfr1-1nfr5-2snf1* infected by *nodC*. (**e**) Thin section of *nfr1-1snf1 nodA* nodule shown in (**c**), r: root, i: infected cell. (**f**) Thin section of *nfr1-1nfr5-2 snf1* nodule infected by *nodC*. Double arrowhead: intercellular bacteria, i: infected cell, arrow: newly divided infected cell. (**g**) Higher magnification of a *nodC*-infected cell in an *nfr1-1nfr5-2 snf1*nodule. Arrow: newly divided infected cell. Size bars (**a**, **b**): 1 cm, (**c**): 20 mm, (**d**): 500 µm (**e**) and (**f**): 100 µm, (**g**): 10 µm.

Lys7, *Lys12*, *Lys15* and *Lys20*, were expressed mainly in root and root nodules[46] and are thus candidates for the cortical receptor or receptor components. Involvement of alternative epidermal or cortical NFRs is supported by observations in *Sesbania*, in which root hair infection was stringently dependent on an intact Nod-factor structure, whereas crack entry was less stringently controlled[47,48] but still dependent on continuous Nod-factor synthesis for effective invasion[49]. Furthermore, the suggested cross-signalling through CCaMK and CYCLOPS interaction also seems to be required for nodule infection thread formation following the intercellular infection mode. Absence of intercellular infection in *nfr1-1 snf2*, *nfr5-2 snf2*, *ccamk-13 snf2* and *cyclops snf1* mutants concurs with this interpretation, as does the recent observation of impaired infection thread progression following RNA-mediated interference knockdown of CCaMK in *Sesbania*[50].

Intercellular infection of single cells as observed in, for example, *nfr1 nfr5 snf1* mutants inoculated with the bacterial *nodC* mutant may constitute the ground state of bacterial invasion mobilized during evolution of nodulation. This intercellular process was approximately 20- to 100-fold less effective than normal root hair invasion. Symbiosomes were observed in infected cells, indicating that endocytosis occurred in the absence of Nod-factor and NFR1 and NFR5 receptors. Endocytosis in the apparent absence of local Nod-factor synthesis in cortical infection threads was also observed in mixed inoculation of *Sesbania*[49]. In this context, the lack of infected nodules observed in *symrk snf1* double mutant plants inoculated with *nodC* and *nodA* mutant strains is puzzling. This may suggest that the SYMRK receptor would be necessary for single cell infection in contrast to infection through infection threads. However, the low level of infection by *nodC* and *nodA* mutant strains observed on *nfr1 nfr5 snf1* mutants cautions such a conclusion on the basis of negative results. Considering our positive results with *nodC* and *nodA* infection of *nfr1 nfr5 snf1* mutants, we hypothesize that a capacity for direct intercellular infection may constitute an ancient invasion path that evolved at the emergence of the legume family or maybe at the emergence of the eurosid I clade containing all nodulating plants. Division of primary infected single cells would conceivably lead to the fully infected Nod-factor-independent nodulation observed in *Aeschynomene*-type nodules[1,51]. In a subsequent evolutionary step, the Nod-factor and cortical NFR-dependent crack entry and subsequent cortical infection thread propagation of invasion could have been established. The most highly evolved state envisaged is the root hair infection mode. This infection mode required Nod-factor, epidermal NFR1 and NFR5 receptors, and is predicted to also involve cortical NFRs with less stringency than NFR1 and NFR5 receptors. The ability of *Sesbania* to switch between a root hair infection mode requiring Nod-factor decorations and a crack entry mode less dependent on Nod-factor structure[48] supports our interpretation, as does the infrequent and delayed infection of nodules in a root hairless mutant[52] and rare events in flooded *Lotus* spp[53]. Overall, this model postulates an evolutionary process in which the advanced root hair infection bestowed a set of legume hosts with a tighter and more selective control of bacterial passage through the epidermis (Fig. 6b). Our observations also suggest that alternative invasion modes have been maintained during evolution and that they are not mutually exclusive. Presence of different infection modes in *Sesbania*, *Chamaecrista*[1], and both a Nod-factor-dependent and a Nod-factor-independent mechanism for nodulation in *Aeschynomene sensitiva*[51], is in accordance with these notions. On this basis, we propose that taking non-exclusive infection modes into account may contribute to resolving some of the difficulties in aligning nodule evolution and the legume phylogeny[1]. Further studies of the direct infection pathway(s) will not only impact biotechnological applications and improve our understanding of plant–microbe interactions but may be key to elucidate the evolution of symbiosis.

Methods

Plant material. The *L. japonicus* mutants used in this study are all in an ecotype Gifu B-129 background[54].

Bacterial strains. For details on *M. loti* strains, see Supplementary Table S2. The identity of bacteria in selected, infected nodules was confirmed by re-isolation of bacteria from surface-sterilized nodules, followed by genotyping by specific PCR. For primers, see Supplementary Table S3.

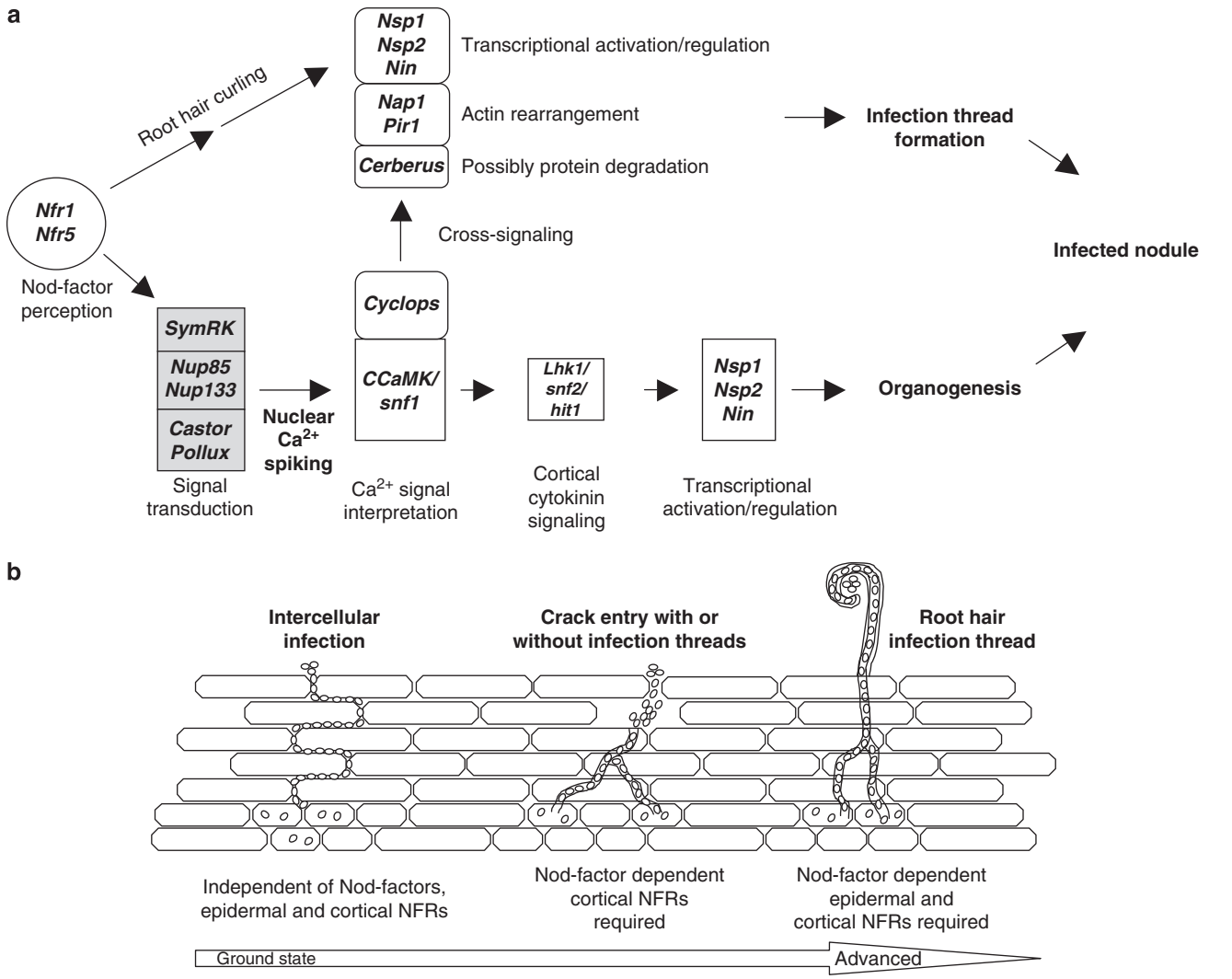

Figure 6 | Model for evolution of legume nodulation and genes assigned to infection thread and organogenic pathways. (**a**) Parallel infection thread and organogenic pathways in wild-type *Lotus*. Cross-signalling through CYCLOPS is indicated. The grey box marks genes that are dispensable for infection thread formation in the *snf1* genetic background. (**b**) Model for molecular evolution of infection pathways in legumes. Intercellular single infection is suggested to be the ground state of rhizobial infection of roots, followed by the crack entry and root hair infection modes. The components of crack entry and single cell infection pathways are less well described and the functional model presented in (**a**) may only partly represent these infection pathways.

Double mutants and plant genotyping. Double, triple and quadruple mutants were obtained by crossing, followed by genotyping of offspring plants. Similarly, the genotypes of mutant plant lines in individual experiments were verified using allele-specific PCR and/or sequencing of PCR-amplified genomic fragments (for primers and conditions, see Supplementary Table S4). The non-nodulating mutants used to establish crack entry, single cell infection and cross-signalling mechanisms (summarized in Fig. 6a,b) carry stable mutations caused by insertion of LORE1 or LORE2 retrotransposons (*symrk-1*, *symrk-3*, *nfr5-2)*, a deletion (*ccamk-13)* or a premature stop codon (*nfr1-1)*. See Supplementary Table S4 for a full list of genotypes of the mutants used in this study.

DNA techniques. The constitutively active T265D variant of the *Lotus* CCaMK gene driven by the native CCaMK promoter was constructed using overlap extension PCR for site-directed mutagenesis of the wild-type CCaMK construct[17] and conventional cloning techniques. The construct complements the nodulation defect in *Lotus ccamk* mutants[17] and causes spontaneous nodulation in the absence of rhizobia. Transgenic hairy roots carrying CCaMKT265D or control wild-type CCaMK genes were produced through *A. rhizogenes* transformation[9].

Plant growth conditions. Seeds of wild type and mutants were surface sterilized for 20 min in a solution of 0.5–1.0% sodium hypochlorite and grown in a 16/8 h day/night regime of 21/16 °C for up to 7 weeks in square Petri dishes on solid 1/4 B&D slants without nitrate, or in Magenta containers (Sigma) on a substrate of Leca (Optiroc) and Vermiculite (3:1 mixture) supplemented with 75 ml of 1/4 B&D medium without nitrate. On plates, the plant roots were shielded from light by using a metal comb fitting the Petri dish and inserting the lower half of the Petri dish into a rack. Plants were grown with or without inoculation with *M. loti* strains (see below).

Nodule counts. Red and white nodules/nodule primordia were counted and photographed using a Zeiss Discovery V8 stereomicroscope.

Infection thread analysis. To visualize infection threads, roots were inoculated with *M. loti* expressing *lacZ* or eGFP reporter genes. Each seedling was inoculated with 150–400 µl (OD600 ~0.01 to 0.02) of *M. loti* expressing the relevant reporter gene and infection threads were visualized at selected time points after inoculation by staining for β-galactosidase activity[8]. After clearing in 30% lactic acid, the roots were mounted on glass slides in glycerol and observed with a bright field Zeiss Axioplan microscope with ×10, ×20 or ×40 objectives, equipped with DIC optics. For eGFP-expressing bacteria, intact roots were mounted on slides in deionized water and observed directly with a Zeiss fluorescence microscope with standard FITC filters. Images were taken with a Zeiss LSM 510 Meta confocal microscope, with excitation at 488 nm, and a BP 505–530 emission filter. Images were recorded with Axiovision software.

The number of infection threads was recorded either per root for short roots or per cm root for older, longer roots. Roots from at least two different plants were scored for each genotype and between 10 and 80 cm roots were inspected for each genotype. The number of infection threads in thin sections was counted in two representative sections of 10 different nodules for each plant genotype.

Microscopy. Nodules were prepared for light and TEM coupled with immunogold labelling with the rat monoclonal antibody MAC236[42] and infection threads from all genotypes were labelled. Nodules that had been fixed in 2.5% glutaraldehyde in 0.1 M sodium cacodylate (pH 7.0) overnight at 4 °C were dehydrated in an ethanol series, and embedded in LR White acrylic resin (Agar Scientific). Semithin sections (1 µm) were taken for light microscopy and ultrathin (70 nm) sections were taken for TEM using a Leica UCT ultramicrotome. The semithin sections were collected on glass slides and stained with 0.1% toluidine blue, whereas the ultrathin sections were collected on pioloform-coated nickel grids and immunogold labelled with the MAC236 antibody. The sections were incubated for 2 h in MAC236 (diluted 1:10), followed by 30 min incubation in an anti-rat secondary antibody raised in rabbit (diluted 1:400) (Southern Biotechnology), and then for 1 h in 15 nm goat anti-rabbit gold (GE Healthcare) (diluted 1:100). The ultrathin sections were then stained with uranyl acetate for 10 min before being viewed and digitally photographed using a JEM 1400 transmission electron microscope (JEOL). Note that bacteria inside *Lotus* infection threads may seem crenellated[53].

References

1. Sprent, J. I. Evolving ideas of legume evolution and diversity: a taxonomic perspective on the occurrence of nodulation. *New Phytol.* **174,** 11–25 (2007).
2. Gage, D. J. Infection and invasion of roots by symbiotic, nitrogen-fixing rhizobia during nodulation of temperate legumes. *Microbiol Mol Biol Rev* **68,** 280–300 (2004).
3. Lerouge, P. *et al.* Symbiotic host-specificity of Rhizobium meliloti is determined by a sulphated and acylated glucosamine oligosaccharide signal. *Nature* **344,** 781–784 (1990).
4. Lopez-Lara, I. M. *et al.* Structural identification of the lipo-chitin oligosaccharide nodulation signals of Rhizobium loti. *Mol. Microbiol.* **15,** 627–638 (1995).
5. Radutoiu, S. *et al.* Plant recognition of symbiotic bacteria requires two LysM receptor-like kinases. *Nature* **425,** 585–592 (2003).
6. Madsen, E. B. *et al.* A receptor kinase gene of the LysM type is involved in legume perception of rhizobial signals. *Nature* **425,** 637–640 (2003).
7. Arrighi, J. F. *et al.* The *Medicago truncatula* lysin motif-receptor-like kinase gene family includes NFP and new nodule-expressed genes. *Plant Physiol.* **142,** 265–279 (2006).
8. Miwa, H., Sun, J., Oldroyd, G. E. & Downie, J. A. Analysis of Nod-factor-induced calcium signaling in root hairs of symbiotically defective mutants of *Lotus japonicus*. *Mol. Plant Microbe Interact.* **19,** 914–923 (2006).
9. Radutoiu, S. *et al.* LysM domains mediate lipochitin-oligosaccharide recognition and Nfr genes extend the symbiotic host range. *EMBO J.* **26,** 3923–3935 (2007).
10. Stracke, S. *et al.* A plant receptor-like kinase required for both bacterial and fungal symbiosis. *Nature* **417,** 959–962 (2002).
11. Endre, G. *et al.* A receptor kinase gene regulating symbiotic nodule development. *Nature* **417,** 962–966 (2002).
12. Ane, J. M. *et al. Medicago truncatula* DMI1 required for bacterial and fungal symbioses in legumes. *Science* **303,** 1364–1367 (2004).
13. Imaizumi-Anraku, H. *et al.* Plastid proteins crucial for symbiotic fungal and bacterial entry into plant roots. *Nature* **433,** 527–531 (2005).
14. Charpentier, M. *et al. Lotus japonicus* CASTOR and POLLUX are ion channels essential for perinuclear calcium spiking in legume root endosymbiosis. *Plant Cell* **20,** 3467–3479 (2008).
15. Kanamori, N. *et al.* A nucleoporin is required for induction of $Ca2^{+}$ spiking in legume nodule development and essential for rhizobial and fungal symbiosis. *Proc. Natl. Acad. Sci. USA* **103,** 359–364 (2006).
16. Saito, K. *et al.* NUCLEOPORIN85 is required for calcium spiking, fungal and bacterial symbioses, and seed production in *Lotus japonicus*. *Plant Cell* **19,** 610–624 (2007).
17. Tirichine, L. *et al.* Deregulation of a Ca^{2+}/calmodulin-dependent kinase leads to spontaneous nodule development. *Nature* **441,** 1153–1156 (2006).
18. Levy, J. *et al.* A putative Ca^{2+} and calmodulin-dependent protein kinase required for bacterial and fungal symbioses. *Science* **303,** 1361–1364 (2004).
19. Mitra, R. M. *et al.* A Ca^{2+}/calmodulin-dependent protein kinase required for symbiotic nodule development: Gene identification by transcript-based cloning. *Proc. Natl. Acad. Sci. USA* **101,** 4701–4705 (2004).
20. Yano, K. *et al.* CYCLOPS, a mediator of symbiotic intracellular accommodation. *Proc. Natl. Acad. Sci. USA* **105,** 20540–20545 (2008).
21. Sieberer, B. J. *et al.* A nuclear-targeted cameleon demonstrates intranuclear Ca2+ spiking in *Medicago truncatula* root hairs in response to rhizobial nodulation factors. *Plant Physiol.* **151,** 1197–1206 (2009).
22. Schauser, L., Roussis, A., Stiller, J. & Stougaard, J. A plant regulator controlling development of symbiotic root nodules. *Nature* **402,** 191–195 (1999).
23. Marsh, J. F. *et al. Medicago truncatula* NIN is essential for rhizobial-independent nodule organogenesis induced by autoactive calcium/calmodulin-dependent protein kinase. *Plant Physiol.* **144,** 324–335 (2007).
24. Smit, P. *et al.* NSP1 of the GRAS protein family is essential for rhizobial Nod factor-induced transcription. *Science* **308,** 1789–1791 (2005).
25. Kalo, P. *et al.* Nodulation signaling in legumes requires NSP2, a member of the GRAS family of transcriptional regulators. *Science* **308,** 1786–1789 (2005).
26. Heckmann, A. B. *et al. Lotus japonicus* nodulation requires two GRAS domain regulators, one of which is functionally conserved in a non-legume. *Plant Physiol.* **142,** 1739–1750 (2006).
27. Murakami, Y. *et al.* Positional cloning identifies *Lotus japonicus* NSP2, a putative transcription factor of the GRAS family, required for NIN and ENOD40 gene expression in nodule initiation. *DNA Res.* **13,** 255–265 (2006).
28. Middleton, P. H. *et al.* An ERF transcription factor in *Medicago truncatula* that is essential for Nod factor signal transduction. *Plant Cell* **19,** 1221–1234 (2007).
29. Asamizu, E., Shimoda, Y., Kouchi, H., Tabata, S. & Sato, S. A positive regulatory role for LjERF1 in the nodulation process is revealed by systematic analysis of nodule-associated transcription factors of *Lotus japonicus*. *Plant Physiol.* **147,** 2030–2040 (2008).
30. Hogslund, N. *et al.* Dissection of symbiosis and organ development by integrated transcriptome analysis of *lotus japonicus* mutant and wild-type plants. *PLoS One* **4,** e6556 (2009).
31. Mitra, R. M., Shaw, S. L. & Long, S. R. Six nonnodulating plant mutants defective for Nod factor-induced transcriptional changes associated with the legume-rhizobia symbiosis. *Proc. Natl. Acad. Sci. USA* **101,** 10217–10222 (2004).
32. Tirichine, L. *et al.* A gain-of-function mutation in a cytokinin receptor triggers spontaneous root nodule organogenesis. *Science* **315,** 104–107 (2007).
33. Murray, J. D. *et al.* A cytokinin perception mutant colonized by rhizobium in the absence of nodule organogenesis. *Science* **315,** 101–104 (2007).
34. Yokota, K. *et al.* Rearrangement of actin cytoskeleton mediates invasion of *Lotus japonicus* roots by *Mesorhizobium loti*. *Plant Cell* **21,** 267–284 (2009).
35. Yano, K. *et al.* CERBERUS, a novel U-box protein containing WD-40 repeats, is required for formation of the infection thread and nodule development in the legume-Rhizobium symbiosis. *Plant J.* **60,** 168–180 (2009).
36. Tirichine, L., James, E. K., Sandal, N. & Stougaard, J. Spontaneous root-nodule formation in the model legume *Lotus japonicus*: a novel class of mutants nodulates in the absence of rhizobia. *Mol. Plant Microbe Interact.* **19,** 373–382 (2006).
37. Gleason, C., Chaudhuri, S., Yang, T., Munoz, A., Poovaiah, B. W. & Oldroyd, G. E. Nodulation independent of rhizobia induced by a calcium-activated kinase lacking autoinhibition. *Nature* **441,** 1149–1152 (2006).
38. Limpens, E. *et al.* Formation of organelle-like N2-fixing symbiosomes in legume root nodules is controlled by DMI2. *Proc. Natl. Acad. Sci. USA* **102,** 10375–10380 (2005).
39. Capoen, W., Goormachtig, S., De Rycke, R., Schroeyers, K. & Holsters, M. SrSymRK, a plant receptor essential for symbiosome formation. *Proc. Natl. Acad. Sci. USA* **102,** 10369–10374 (2005).
40. Messinese, E. *et al.* A novel nuclear protein interacts with the symbiotic DMI3 calcium- and calmodulin-dependent protein kinase of *Medicago truncatula*. *Mol. Plant Microbe Interact.* **20,** 912–921 (2007).
41. Rodpothong, P. *et al.* Nodulation gene mutants of *Mesorhizobium loti* R7A-nodZ and nolL mutants have host-specific phenotypes on Lotus spp. *Mol. Plant Microbe Interact.* **22,** 1546–1554 (2009).
42. James, E. K., Minchin, F. R., Iannetta, P. P. M. & Sprent, J. I. Temporal relationships between nitrogenase and intercellular glycoprotein in developing white lupin nodules. *Ann. Bot.* **79,** 493–503 (1997).
43. Gonzalez-Sama, A., Lucas, M. M., de Felipe, M. R. & Pueyo, J. J. An unusual infection mechanism and nodule morphogenesis in white lupin (Lupinus albus). *New Phytol* **163,** 371–380 (2004).
44. Esseling, J. J., Lhuissier, F. G. P. & Emons, A. M. C. A nonsymbiotic root hair tip growth phenotype in NORK-mutated legumes: Implications for nodulation factor-induced signaling and formation of a multifacetted root hair pocket for bacteria. *Plant Cell* **16,** 933–944 (2004).
45. D'Haeze, W. *et al.* Roles for azorhizobial nod factors and surface polysaccharides in intercellular invasion and nodule penetration, respectively. *Mol. Plant Microbe Interact.* **11,** 999–1008 (1998).
46. Lohmann, G. V. *et al.* Evolution and regulation of the *Lotus japonicus* LysM receptor gene family. *Mol. Plant Microbe Interact.* **23,** 510–521 (2010).
47. D'Haeze, W., Mergaert, P., Prome, J. C. & Holsters, M. Nod factor requirements for efficient stem and root nodulation of the tropical legume Sesbania rostrata. *J. Biol. Chem.* **275,** 15676–15684 (2000).
48. Goormachtig, S., Capoen, W., James, E. K. & Holsters, M. Switch from intracellular to intercellular invasion during water stress-tolerant legume nodulation. *Proc. Natl. Acad. Sci. USA* **101,** 6303–6308 (2004).
49. Den Herder, J. V. C., De Rycke, R., Corich, V., Holsters, M. & Goormachtig, S. Nod factor perception during infection thread growth fine-tunes nodulation. *Mol. Plant Microbe Interact.* **20,** 129–137 (2007).
50. Capoen, W. *et al.* Calcium spiking patterns and the role of the calcium/calmodulin-dependent kinase CCaMK in lateral root base nodulation of Sesbania rostrata. *Plant Cell* **21,** 1526–1540 (2009).
51. Giraud, E. *et al.* Legumes symbioses: absence of Nod genes in photosynthetic bradyrhizobia. *Science* **316,** 1307–1312 (2007).

52. Karas, B. *et al.* Invasion of *Lotus japonicus* root hairless 1 by *Mesorhizobium loti* involves the nodulation factor-dependent induction of root hairs. *Plant Physiol.* **13,** 1331–1344 (2005).
53. James, E. K. & Sprent, J. I. Development of N_2-fixing nodules on the wetland *Lotus uliginosus* exposed to conditions of flooding. *New. Phytol.* **142,** 219–231 (1999).
54. Handberg, K. & Stougaard, J. *Lotus-Japonicus*, an autogamous, diploid legume species for classical and molecular-genetics. *Plant J.* **2,** 487–496 (1992).

Acknowledgments

The Danish National Research Foundation funded this study. We thank Nick Brewin for the MAC236 antibody, Krzysztof Szczyglowski for *hit1* seeds and Masayoshi Kawaguchi for *nup85* seeds.

Author contributions

L.H.M., L.T., A.J. and A.B.H. isolated and characterized the synthetic mutants. A.J., A.S.B., E.K.J. and L.H.M. performed the microscopy. J.T.S. and C.W.R. constructed the *M. loti* mutants, L.T. observed the first partially infected nodules and initiated the work using synthetic mutants. J.S. coordinated and wrote the paper.

Author information

Supplementary Information accompanies this paper on http://www.nature.com/naturecommunications.

Competing financial interests: The authors have no competing interests as defined by Nature Publishing Group, or other interests that might be perceived to influence the results and/or discussion reported in this article.

Reprints and permission information is available online at http://npg.nature.com/reprintsandpermissions/

How to cite this article: Madsen, L.H. *et al.* The molecular network governing nodule organogenesis and infection in the model legume *Lotus japonicus*. *Nat. Commun.* 1:10 doi: 10.1038/ncomms1009 (2010).